



HAL
open science

Large-Signal Average Modeling of Two Decentralized Distributed Generations Based on Boost Converter

Roghayeh Gavagsaz-Ghoachani, Matheepot Phattanasak, Mohammad Afkar,
Ehsan Jamshidpour, Serge Pierfederici

► **To cite this version:**

Roghayeh Gavagsaz-Ghoachani, Matheepot Phattanasak, Mohammad Afkar, Ehsan Jamshidpour, Serge Pierfederici. Large-Signal Average Modeling of Two Decentralized Distributed Generations Based on Boost Converter. 23rd International Conference on Environment and Electrical Engineering (EEEIC 2023), IEEE, Jun 2023, Madrid, Spain. 10.1109/EEEIC/ICPSEurope57605.2023.10194681 . hal-04137336

HAL Id: hal-04137336

<https://hal.univ-lorraine.fr/hal-04137336>

Submitted on 22 Jun 2023

HAL is a multi-disciplinary open access archive for the deposit and dissemination of scientific research documents, whether they are published or not. The documents may come from teaching and research institutions in France or abroad, or from public or private research centers.

L'archive ouverte pluridisciplinaire **HAL**, est destinée au dépôt et à la diffusion de documents scientifiques de niveau recherche, publiés ou non, émanant des établissements d'enseignement et de recherche français ou étrangers, des laboratoires publics ou privés.

Large-Signal Average Modeling of Two Decentralized Distributed Generations Based on Boost Converter

Roghayeh Gavagsaz-Ghoachani
*Mechanical and Energy Engineering
 Department of Renewable energy
 Shahid Beheshti University
 Tehran, Iran
 r_gavagsaz@sbu.ac.ir*

Matheepot Phattanasak
*Department of Teacher Training
 in Electrical Engineering
 King Mongkut's University
 of Technology North Bangkok
 Bangkok, Thailand
 matheepot.p@fte.kmutnb.ac.th*

Mohammad Afkar
*Mechanical and Energy Engineering
 Department of Renewable energy
 Shahid Beheshti University
 Tehran, Iran
 mo.afkar@mail.sbu.ac.ir*

Ehsan Jamshidpour
*Université de Lorraine-GREEN
 F-54000, Nancy, France
 ehsan.jamshidpour@univ-lorraine.fr*

Serge Pierfederici
*Université de Lorraine-Lemta
 F-54000, Nancy, France
 serge.pierfederici@univ-lorraine.fr*

Abstract—This paper presents a study on the stability of a DC microgrid system, focusing on the development of an average model. The system includes two distributed generations (DGs) based on the boost converter. The model is developed by considering the differential equations of the system, including the power circuits and controllers. Three types of controllers are used in the study, namely the indirect sliding mode controller, the energy controller, and the droop controller. The droop controller is responsible for sharing the current between the DGs. The simulation of the system is performed using MATLAB/Simulink software, and the results obtained from the developed model are compared in two scenarios. In addition, the study examines the effect of the droop parameter on the system's stability.

Index Terms—averaged model, decentralize, distributed generation, microgrid

I. INTRODUCTION

As the need for primary energy is increasing, while non-renewable energy resources are limited, and the environmental challenges related to the mentioned resources have promoted the use of renewable energy as an appropriate solution to the aforementioned problems. [1]. The renewables resources are used in distributed power generation systems and microgrids. To control microgrids, different methods are proposed in the literature [2]–[7].

In [8] a decentralized passivity-based control is proposed for a system which is shown in Fig.1 in order to guarantee the stability of the system. The system consists of two distributed generations which are connected to DC bus through the two three-level boost converters to supply a resistive load [9].

To apply any control method, the system including the boost converters must be studied through mathematical model [10].

There are two types of analytical models, which are discrete and average models. Usually, for simplicity, the model based on the average approach is considered to study the system's behavior [11]. In this paper, the stability of the same system presented in [8], which is controlled by a sliding mode controller, is studied. The stability of the system is verified by computing the eigenvalues of the Jacobian matrix obtained using MATLAB software. To find this Jacobian matrix of the system, a large-signal model of the system is presented and the accuracy of this model is validated.

The organization of this as follows. The considered system, the differential equations, and the used controller will be detailed in Section II. The system will be presented using the large-signal model in Section III. In Section IV, to validate the considered average model, the results from a simulation using

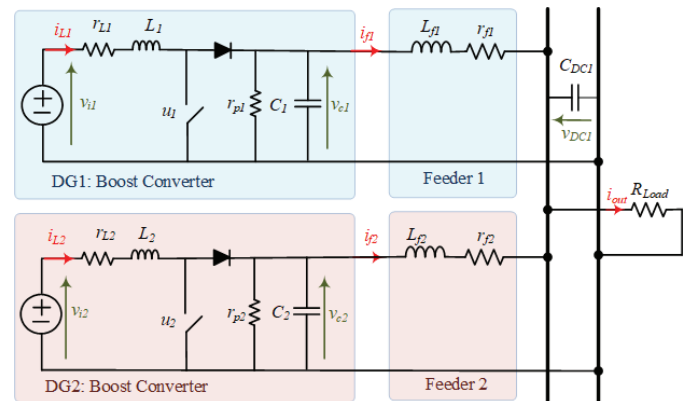


Fig. 1. Studied system.

MATLAB/Simulink will be given. In section V, conclusions are given.

II. STUDIED DISTRIBUTED GENERATION SYSTEM

In this section, the behaviors of the studied system, represented in Fig. 1, are detailed using the differential equations of state.

A. Power converters and feeding cables

In this section, the investigated system (Fig. 1), is presented. There are two DGs. Both DGs are represented by DC-DC boost converters. The state equations are used to explain the behaviors of the system can be expressed as:

$$\begin{cases} \frac{di_{L1}}{dt} = \frac{1}{L_1} (V_{i1} - r_{L1} i_{L1} - (1 - u_1) v_{c1}) \\ \frac{dv_{c1}}{dt} = \frac{1}{C_1} ((1 - u_1) i_{L1} - i_{f1}) \end{cases} \quad (1)$$

The differential equations of DG2 can be written as:

$$\begin{cases} \frac{di_{L2}}{dt} = \frac{1}{L_2} (V_{i2} - r_{L2} i_{L2} - (1 - u_2) v_{c2}) \\ \frac{dv_{c2}}{dt} = \frac{1}{C_2} ((1 - u_2) i_{L2} - i_{f2}) \end{cases} \quad (2)$$

Suppose that the studied converter is functioned in a Continuous-Conduction Mode (CCM). The input voltages (V_{i1} , V_{i2}) for both DGs are constant.

For the feeding cable, the currents flowing through the line feeding the power from DG1 and DG2 (Feeder1 and Feeder2 in Fig.1) to load including DC bus capacitor voltage can be presented as:

$$\begin{cases} \frac{di_{f1}}{dt} = \frac{1}{L_{f1}} (v_{c1} - r_{f1} i_{f1} - v_{DC}) \\ \frac{di_{f2}}{dt} = \frac{1}{L_{f2}} (v_{c2} - r_{f2} i_{f2} - v_{DC}) \\ \frac{dv_{DC}}{dt} = \frac{1}{C_{DC}} (i_{f1} + i_{f2} - i_{out}) \end{cases} \quad (3)$$

where $i_{out} = v_{DC}/R_{out}$, L_{f1}, r_{f1} are the inductance and the resistance of the Feeder1, and L_{f2}, r_{f2} are the inductance and the resistance of the Feeder2.

B. Control system

1) *Current control*: To control the inductor currents, the sliding-mode controller with indirect approach [9] for DG is used and it is depicted in Fig.2. For the studied system, there are two currents, therefore, the two sliding surfaces are proposed. Both chosen sliding surfaces for the inductor current L_1 and L_2 are S_{i1} and S_{i2} . These surfaces (equations (4)) are used to govern the inductor currents (i_{L1} and i_{L2}).

$$\begin{cases} S_{i1} = i_{L1} - i_{ref1} + K_{i1} \int (i_{L1} - i_{ref1}) dt \\ S_{i2} = i_{L2} - i_{ref2} + K_{i2} \int (i_{L2} - i_{ref2}) dt \end{cases} \quad (4)$$

The reaching law $\dot{S} = -\lambda S$ is utilized to govern the two equations listed in equations (5). The presented equations are used to solve the duty cycles of the two boost converters (d_1 and d_2). Utilizing fixed-switching frequency pulse-width modulator, the switching control signal is obtained. The used controller for both DGs are illustrated as block diagrams in

Fig. 2. The parameters K_{i1} , K_{i2} , λ_{i1} , and λ_{i2} allowing to set the bandwidth of the current control loop [12].

$$\begin{cases} \dot{S}_{i1} = -\lambda_{i1} S_{i1} \\ \dot{S}_{i2} = -\lambda_{i2} S_{i2} \end{cases} \quad (5)$$

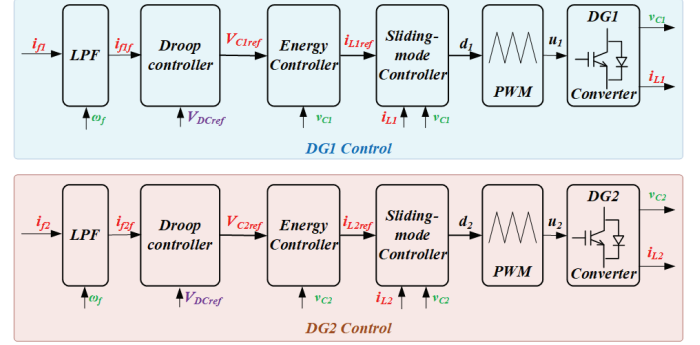


Fig. 2. Controller for the DGs.

2) *Voltage control*: The output voltage v_{c1} and v_{c2} are controlled by controlling their energy ($y = \frac{1}{2} C v_c^2$). The energy controller for both DGs is similar, therefore, here, only for DG1 is presented. The controller is defined as :

$$\begin{aligned} \vartheta &= \dot{y}_{1ref} - \dot{y}_1 + 2\xi\omega_n (y_{1ref} - y_1) \\ &+ \omega_n^2 \int (y_{1ref} - y_1) d\tau = 0 \end{aligned} \quad (6)$$

where ξ is damping ratio, ω_n is controlled bandwidth. The current reference i_{1ref} can be found using equation (7).

$$i_{1ref} V_{i1} - (\dot{y} + i_{f1} v_{c1} + r_{L1} i_{1ref}^2) = 0 \quad (7)$$

To apply the droop controller, one can implement it by modifying the reference voltage of the output capacitor v_{c1ref} and v_{c2ref} . It depends on a proportion of the actual feeding current and the given nominal feeding current (I_{f1N} , I_{f2N}):

$$\begin{cases} v_{c1ref} = V_{DCref} - \Delta V \left(\frac{i_{f1f}}{I_{f1N}} - 1 \right) \\ v_{c2ref} = V_{DCref} - \Delta V \left(\frac{i_{f2f}}{I_{f2N}} - 1 \right) \end{cases} \quad (8)$$

where ΔV is the droop parameter, V_{DCref} the output capacitor voltage reference, I_{f1N} , I_{f2N} the nominal load current of both distributed generators, respectively. i_{f1f} and i_{f2f} are the filtered currents thanks to the low-pass filter with a cutoff frequency ω_f . Suppose that $i_{f1f} = i_{f1} \approx \text{constant}$ and $i_{f2f} = i_{f2} \approx \text{constant}$.

III. AVERAGE MODEL

The whole system is presented in this section using an average model. The proposed model will be given and then the equilibrium point corresponding to physical circuit and its specification would be given for each converter as well as the feeding cables.

A. Studied model

Using the information of the system and the controller detailed earlier, the state vector $X \in \mathbb{R}^{13}$ is given as:

$$X = \begin{bmatrix} X_A \\ X_B \end{bmatrix} \quad (9)$$

where vector $X_A \in \mathbb{R}^9$ is the state variables and the vector $X_B \in \mathbb{R}^4$ is the controllers' variables as follows:

$$[X_A] = \begin{bmatrix} X_1 \\ X_2 \\ X_3 \\ X_4 \\ X_5 \\ X_6 \\ X_7 \\ X_8 \\ X_9 \end{bmatrix} = \begin{bmatrix} \overline{i_{L1}} \\ \overline{i_{L2}} \\ \overline{v_{C1}} \\ \overline{v_{C2}} \\ \overline{v_{DC}} \\ \overline{i_{f1}} \\ \overline{i_{f2}} \\ \overline{i_{f1f}} \\ \overline{i_{f2f}} \end{bmatrix} \quad (10)$$

where the symbolization \overline{x} signifies the average quantity of the variable x considered on the considered one switching cycle.

$$[X_B] = \begin{bmatrix} X_{10} \\ X_{11} \\ X_{12} \\ X_{13} \end{bmatrix} = \begin{bmatrix} \int (i_{L1} - i_{ref1}) dt \\ \int (i_{L2} - i_{ref2}) dt \\ \int (y_1 - y_{1ref}) dt \\ \int (y_2 - y_{2ref}) dt \end{bmatrix} \quad (11)$$

In (10), this model considers the state variables ($X_1 - X_7$), the augmented variables (filtered variables $X_8 - X_9$), including the variables for the controller (integral components $X_{10} - X_{13}$).

Using the duty cycles and values necessary required from the system equations, the state vector X verifies the equation \dot{X} given in (12) and (1).

$$\dot{X} = H(X) \quad (12)$$

$$[\dot{X}] = \begin{bmatrix} \frac{(-r_{L1}X_1 + V_{i1} - (1-d_1)X_3)}{L_1} \\ \frac{(-r_{L2}X_2 + V_{i2} - (1-d_2)X_4)}{L_2} \\ \frac{(X_1(1-d_1) - X_6)}{C_1} \\ \frac{(X_2(1-d_2) - X_7)}{C_2} \\ \frac{(X_6 + X_7 - i_{out})}{C_{DC}} \\ -\omega_f X_8 + \omega_f X_6 \\ -\omega_f X_9 + \omega_f X_7 \\ \frac{(X_3 - r_{Line1}X_6 - X_5)}{L_{line1}} \\ \frac{(X_4 - r_{Line2}X_7 - X_5)}{L_{line2}} \end{bmatrix} \quad (13)$$

The stability of the average model at the neighborhood of the considered operating point could be investigated through the obtained eigenvalues of mentioned matrix $H(X_0)$.

B. Equilibrium point calculation

To obtain the eigenvalues at an equilibrium point for the considered system, the information of the chosen equilibrium point should be given. Considering the circuit in Fig.2, supposing that all switch devices are ideal, to investigate the system's stability, we need to do the model. Then, a stability analysis

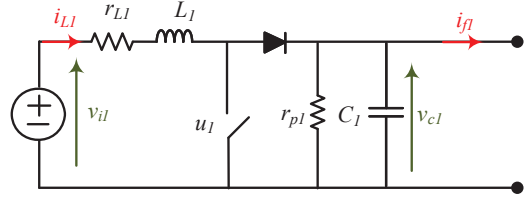


Fig. 3. Boost converter of the studied system.

should be done under a specific operating point. Therefore, calculation of the value of the state variables at the considered operating point is necessary. We can start to calculate the state variable of the considered converter shown in Fig. 3. Using a power balance concept for the considered circuit and supposing that the parasitic resistance of the output capacitor $r_{p1} = \infty$, we can express the following equation:

$$-v_{i1}i_{L1} + r_{L1}i_{L1}^2 + v_{C1}i_{f1} = 0 \quad (14)$$

Therefore, the current i_{L1} can be found as:

$$i_{L1} = \frac{2P_{in1_{max}}}{V_{i1}} \left(1 - \sqrt{1 - \frac{v_{C1}i_{f1}}{P_{in1_{max}}}} \right) \quad (15)$$

It should be noted that the solution of (14) consists of two parts. But due to the physical circuit where the inductor current can be only positive, the possible inductor current is given in (15). Using (15), one can imply the inductor current for the second source as:

$$i_{L2} = \frac{2P_{in2_{max}}}{V_{i2}} \left(1 - \sqrt{1 - \frac{v_{C2}i_{f2}}{P_{in2_{max}}}} \right) \quad (16)$$

Now, considering $r_{p1} < \infty$, the following equation can be expressed:

$$-v_{i1}i_{L1} + r_{L1}i_{L1}^2 + v_{C1}i_{f1} + \frac{v_{C1}^2}{r_{p1}} = 0 \quad (17)$$

Therefore, the current i_{L1} can be found as:

$$i_{L1} = \frac{2P_{in1_{max}}}{V_{i1}} \left(1 - \sqrt{1 - \frac{v_{C1} \left(i_{f1} + \frac{v_{C1}}{r_{p1}} \right)}{P_{in1_{max}}}} \right) \quad (18)$$

It can be also for the current i_{L2}

$$i_{L2} = \frac{2P_{in2_{max}}}{V_{i2}} \left(1 - \sqrt{1 - \frac{v_{C2} \left(i_{f2} + \frac{v_{C2}}{r_{p2}} \right)}{P_{in2_{max}}}} \right) \quad (19)$$

If the two considered converters are controlled to provide the output capacitor voltage that follows their reference signal well, the output voltages can be considered as constant voltage sources V_{o1} and V_{o2} for simplicity. This results in a simple

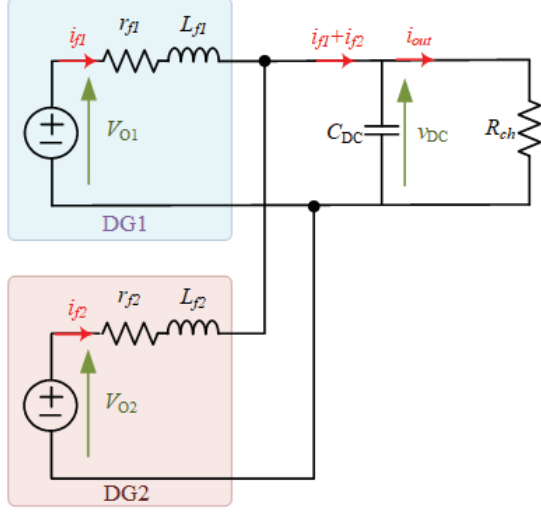


Fig. 4. Simplified studied system.

circuit, as shown in Fig.4. The average currents flowing through the inductors (i_{f1}, i_{f2}) in steady state can be found using KVL's law:

$$\begin{cases} -V_{o1} + r_{Line1}i_{f1} + R_{ch}(i_{f1} + i_{f2}) = 0 \\ -V_{o2} + r_{Line2}i_{f2} + R_{ch}(i_{f1} + i_{f2}) = 0 \end{cases} \quad (20)$$

The load voltage v_{ch} is given by

$$v_{ch} = (i_{f1} + i_{f2}) R_{ch} \quad (21)$$

The voltage across C_{DC} is controlled in order to track its reference voltage V_{DCref} . It is used for the droop voltage controller to adjust the output capacitor voltage reference of the j th boost converter as:

$$v_{orefj} = V_{DCref} - \Delta V \left(\frac{i_{ffj}}{I_{FNj}} - 1 \right) \quad (22)$$

The current i_{ffj} , $j = \{1, 2\}$ is the filtered current, which is filtered using a low-pass filter characterized by a bandwidth of ω_f .

$$\frac{i_{ffj}(s)}{i_{fj}(s)} = \frac{\omega_f}{s + \omega_f} \quad (23)$$

The droop parameters are the voltage ΔV , the nominal load current I_{FNj} , $j = \{1, 2\}$, and the cutoff frequency of the filter ω_f . By replacing v_{C1} in (18) with v_{oref1} and embedding the filter in (23), the current i_{L1} can be obtained. This can also be done for i_{L2} .

The voltages v_{o1} and v_{o2} in (20) must also be replaced by v_{orefj} detailed in (22) to include an effect, which will be occurred from the droop controller concerning the droop parameters and the load current.

IV. SIMULATION RESULTS

To validate the presented large-signal model, some simulation is done in MATLAB/Simulink environment. The parameters of the system that used for these simulations are presented in Table I.

TABLE I
SPECIFICATION AND PARAMETERS

Parameters	Quantity	Value
V_{i1}, V_{i2}	Voltage source	60 V
L_1, L_2	Inductance	1000 μ H
r_1, r_2	Resistance of inductor	300 m Ω
C_1, C_2	Capacitance for each DG	1100 μ F
C_{DC}	DC bus capacitance	100 nF
L_{line1}, L_{line2}	Cable inductance	1 mH
r_{line1}, r_{line2}	Cable resistance	0.1 Ω
f_s	Switching frequency	10 kHz
R_{out}	Load resistance	37.50 Ω
V_{DCref}	DC bus voltage reference	150 V
K_{i1}, K_{i2}	Control parameter	3.14 krad/s
$\lambda_{i1}, \lambda_{i2}$	Control parameter	3.14 krad/s
ω_n	Control parameter	314 rad/s
ξ	Control parameter	0.707
ΔV	Droop parameter	5 V
ω_f (Case I)	Droop parameter (cutoff frequency)	5 rad/s
ω_f (Case II)	Droop parameter(cutoff frequency)	100 rad/s
I_{f1N}	Droop parameter (DG output current)	4 A
I_{f2N}	Droop parameter (DG output current)	4.001 A

In these simulations, two scenarios are considered as follows:

- 1) when the considered system operates stable.
- 2) when the considered system is unstable.

The stability of the system is verified by calculating the eigenvalues of the established Jacobian matrix. These two Cases will be presented in following.

A. Case I: Stable operation condition

Fig. 5 - Fig. 7 present simulations results when the system is stable using the parameters listed in Table I. The current waveforms i_{L1} , i_{L2} (inductor currents) and the voltage waveforms of capacitors v_{C1} , v_{C2} and, V_{CDC} are shown in Fig. 5. The output current for each DG flowing through the cables are shown in Fig. 6. The results of the simulation show that all the currents and voltages in the system follow their reference value and have a correct final value. This means that the system is working in a stable condition. The eigenvalues corresponding to the simulation results are given in Fig. 7. As can be seen, all eigenvalues are in the left half-plane, which confirms that the system is stable.

B. Case II: Unstable operation condition

In the second scenario, the operating point is change to have an unstable operation condition. To do this, the parameter of the droop controller; cutoff frequency (ω_f) can be modified. For the following simulation, a variation of the cutoff frequency (ω_f) is considered, as it shown in the Table I. The simulation results are presented in Fig. 8- Fig. 10.

The inductor current waveforms i_{L1} , i_{L2} and the voltage waveforms of capacitors v_{C1} , v_{C2} and, V_{CDC} are shown in

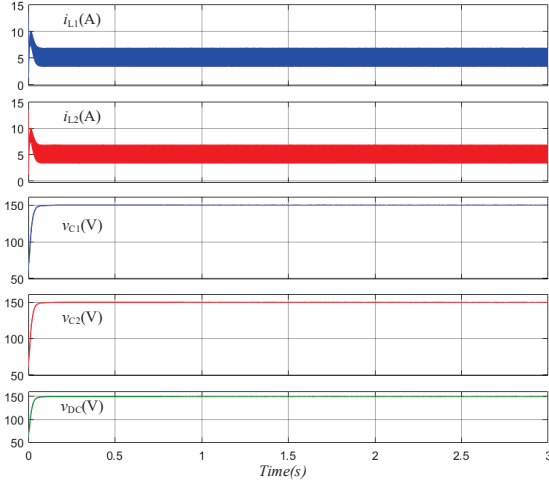


Fig. 5. Up to down; Inductor's currents (i_{L1} , i_{L2}), capacitor's voltages v_{C1} , v_{C2} , v_{CDC} when the system is stable.

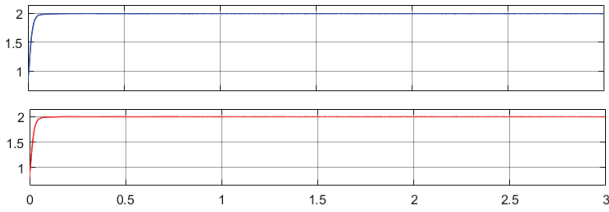


Fig. 6. Output currents of DGs (i_{f1} , i_{f2}) when the system is stable.

Fig. 8. The output current for each DG flowing along the lines are illustrated in Fig. 9. As it is clearly seen on these simulation results, there are an important oscillation on the currents and voltages waveforms. Therefore, the system is unstable. The eigenvalues relating to the obtained simulation results are illustrated in Fig. 10. Obviously, some eigenvalues are migrated to the right-half plane as it can be seen in the zoom window of Fig. 10. Therefore, the system is unstable.

V. CONCLUSION

A model based on an average model for a distributed power generation system consisting of two DGs, using two boost converters is presented in this paper. The system is modeled by the system of differential equations, including three controllers for each DG. To confirm the validity of the proposed model, some simulation tests are performed using MATLAB/Simulink software for two cases in terms of system stability. The first case is when the system is stable and the second case is when the system is unstable. The results obtained from the simulations confirmed the precision of the proposed average model. Additionally, the eigenvalues for the system were calculated, and it was verified that they remain in the left

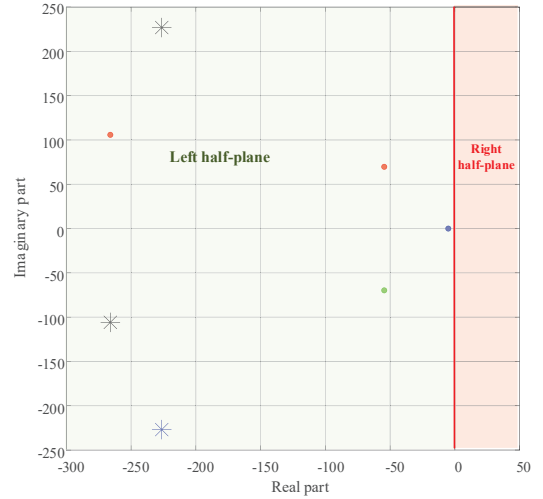
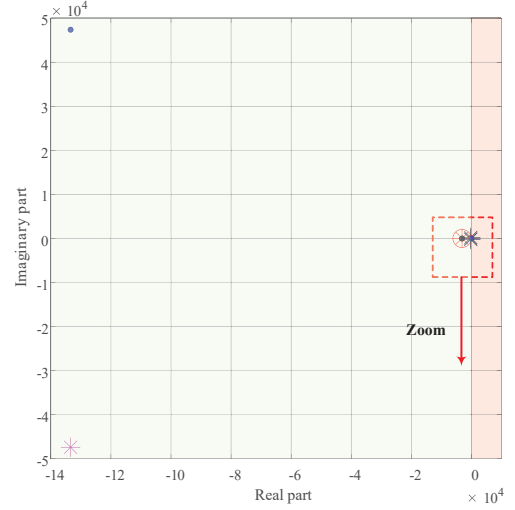


Fig. 7. Top: Eigenvalues when the system is stable, Bottom: Zoomed-in view of the eigenvalues around the origin (point (0,0))

half-plane when the system is stable. A pair of eigenvalues moves to the right half-plane of the s-plane corresponding to the system is unstable. These changes depend on the droop parameters, which is the cutoff frequency (ω_f).

ACKNOWLEDGEMENT

This work was supported in part by an International Research Partnership "Electrical Engineering – Thai French Research Center (EE-TFRC)" under the project framework of the Lorraine Université d'Excellence (LUE) in cooperation between Université de Lorraine and King Mongkut's University of Technology North Bangkok and in part by Shahid Beheshti G.C. University and was funded by National Science, Research and Innovation Fund (NSRF), and King Mongkut's University of Technology North Bangkok with Contract no. KMUTNB-FF-67-B-08.

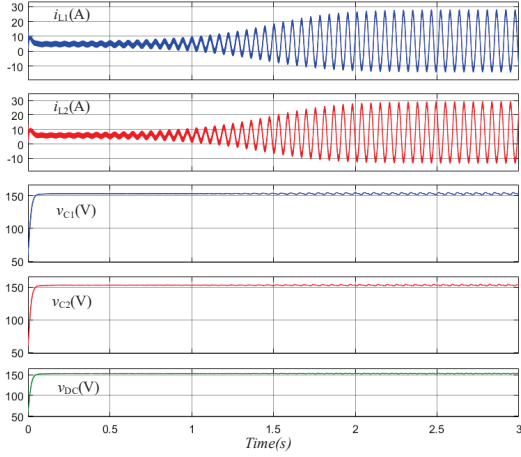


Fig. 8. Up to down ; Inductor's currents (i_{L1} , i_{L2}), capacitor's voltages v_{C1} , v_{C2} , v_{CDC} when the system is unstable.

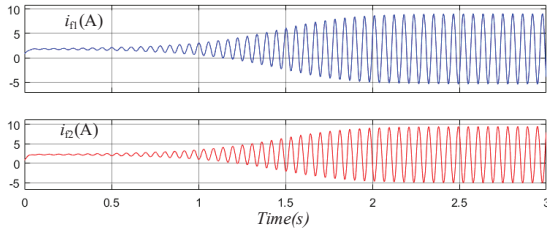


Fig. 9. Output currents of DGs (i_{f1} , i_{f2}) when the system is unstable.

REFERENCES

- [1] T. Alghamdi, D. Said, and H. Mouftah, "Profit maximization for evse-based renewable energy sources in smart cities with different arrival rate scenarios," *IEEE Access*, vol. 9, pp. 58 740–58 754, 2021.
- [2] M. Cucuzzella, K. C. Kosaraju, and J. M. A. Scherpen, "Voltage control of dc microgrids: Robustness for unknown zip-loads," *IEEE Control Systems Letters*, vol. 7, pp. 139–144, 2023.
- [3] K. Dey and A. M. Kulkarni, "Passivity-based decentralized criteria for small-signal stability of power systems with converter-interfaced generation," *IEEE Transactions on Power Systems*, pp. 1–14, 2022.
- [4] P. Thonthong, P. Mungporn, S. Pierfederici, D. Guilbert, N. Takorabet, B. Nahid-Mobarakkeh, Y. Hu, N. Bizon, Y. Huangfu, P. Kumam, and P. Burikham, "Robust hamiltonian energy control based on lyapunov function for four-phase parallel fuel cell boost converter for dc microgrid applications," *IEEE Transactions on Sustainable Energy*, vol. 12, no. 3, pp. 1500–1511, 2021.
- [5] J. Liu, Z. Liu, W. Chen, and H. Su, "Passivity-based control for interleaved double dual boost converters in dc microgrids supplying constant power loads," *IEEE Transactions on Transportation Electrification*, vol. 8, no. 2, pp. 1642–1655, 2022.
- [6] M. A. Hassan, C.-L. Su, F.-Z. Chen, and K.-Y. Lo, "Adaptive passivity-based control of a dc–dc boost power converter supplying constant power and constant voltage loads," *IEEE Transactions on Industrial Electronics*, vol. 69, no. 6, pp. 6204–6214, 2022.
- [7] M. A. Hassan, E.-P. Li, and S. Chi, "Passivity-based control of dc-dc boost power converter for mppt used in dc microgrid systems," in *2018 2nd IEEE Conference on Energy Internet and Energy System Integration (EI2)*, 2018, pp. 1–6.
- [8] M. Afkar, R. Gavagsaz-Ghoachani, M. Phattanasak, and S. Pierfederici, "Decentralized passivity-based control of two distributed generation units in dc microgrids," in *2023 8th International Conference on*

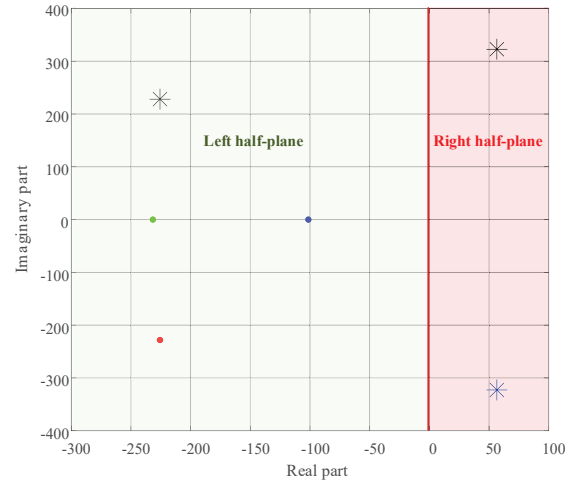
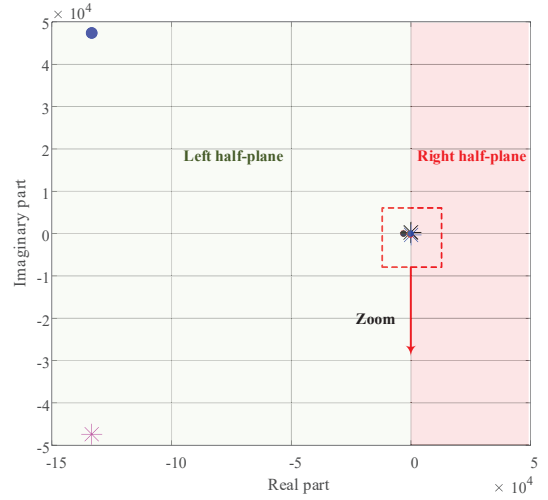


Fig. 10. Top: Eigenvalues when the system is unstable, Bottom: Zoomed-in view of the eigenvalues around the origin (point (0,0))

- Technology and Energy Management (ICTEM)*. IEEE, 2023, pp. 1–5.
- [9] M. Afkar, M. Jebreilzadeh, R. Gavagsaz-Ghoachani, M. Phattanasak, and S. Pierfederici, "A proposed configuration based on three-level boost converter for unbalancing voltage issue in photovoltaic systems operation," in *ICREDG 2019*. IEEE, 2019.
- [10] R. Gavagsaz-Ghoachani, M. Phattanasak, J. Martin, S. Pierfederici, B. Nahid-Mobarakkeh, and P. Riedinger, "A lyapunov function for switching command of a dc–dc power converter with an lc input filter," *IEEE Transactions on Industry Applications*, vol. 53, no. 5, pp. 5041–5050, 2017.
- [11] A. Villarruel-Parra and A. J. Forsyth, "Enhanced average-value modeling of interleaved dc–dc converters using sampler decomposition," *IEEE Transactions on Power Electronics*, vol. 32, no. 3, pp. 2290–2299, 2017.
- [12] A. Battiston, E.-H. Miliani, J.-P. Martin, B. Nahid-Mobarakkeh, S. Pierfederici, and F. Meibody-Tabar, *A Control Strategy for Electric Traction Systems Using a PM-Motor Fed by a Bidirectional Z-Source Inverter*, 2014, vol. 63, no. 9.